

Recursive Fuzzy Operator for Contrast Enhancement of Digital Color Images

Fabrizio Russo

Abstract— A new method for contrast enhancement of RGB color images is presented in this paper. The approach is based on a three-output recursive operator that adopts fuzzy relations in order to perform detail sharpening and noise reduction as well. The optimal amounts of sharpening and smoothing can be easily achieved by choosing a set of parameter values. Results of computer simulations dealing with color pictures corrupted by Gaussian noise show that the proposed method is very effective. It can sharpen the details of a color image and reduce the noise.

Keywords— image processing, image enhancement, image sharpening, nonlinear filters, fuzzy models.

I. INTRODUCTION

TECHNIQUES for contrast enhancement are widely adopted in a number of research and application areas where digital images have rapidly become the most important source of information such as medical systems, remote sensing, video surveillance, biometrics and robotics. Since contrast enhancement can highlight important features embedded in the image data, it can improve the accuracy of subsequent operations devoted to parameter estimation, object recognition and scene interpretation. Contrast enhancement is also typically adopted in consumer electronics dealing with digital cameras and camcorders in order to improve the visual quality of still images and video sequences. The noise increase possibly produced by the sharpening process, however, is a very important problem in the design of any image enhancement system. A classical example of this annoying effect is offered by the linear *unsharp masking* (UM) method [1-2]. In this technique, a fraction of the high-pass filtered image is added to the original data and the resulting effect is edge enhancement and noise amplification. In order to solve this problem, more advanced approaches have adopted nonlinear algorithms that can limit the noise increase during detail sharpening [3-7]. As an example, very interesting results were obtained using weighted medians (WM) and permutation weighted medians (PWMs) instead of high-pass linear filters in the UM scheme [8-10]. Polynomial UM methods such as the Teager-based operator [11-12] and the cubic UM method [13-14] were also proposed in order to control the noise amplification. Nonlinear techniques such as the rational UM

operators can avoid noise increase and excessive overshoot on object contours too [15]. Nonlinear methods based on piecewise linear functions have also been proposed for the enhancement of noisy images [16-17]. As a key feature, these techniques offer a very easy control of the sharpening and smoothing effects. Other methods combining sharpening and noise reduction are available in the literature: they include techniques adopting bilateral filtering [18], non-local means (NLM) [19] and anisotropic diffusion for the processing of grayscale [20] and color pictures [21-22]. In this framework, contrast enhancement approaches that try to avoid color distortion have been proposed in [23-25]. Fuzzy models too are a powerful resource for contrast enhancement of noisy images. Indeed, fuzzy set-based techniques are well suited to address the uncertainty that typically occurs when conflicting tasks must be combined, for example, sharpening and noise reduction [26-27].

In this paper we present a novel fuzzy method for the enhancement of noisy color pictures that extends and improves our previous techniques for grayscale images. The proposed approach consists in a three-output operator that combines sharpening and noise reduction of RGB data by resorting to simple fuzzy relations. In order to preserve the chroma information, the sharpening is applied to luminance only. The method is recursive and operates on pixel patterns of appropriate shapes in order to limit image distortion. The resulting behavior of the operator can be finely adapted to the specific needs by choosing a set of parameter values. The parameter tuning is not a critical process and a satisfactory behavior can be easily achieved by adopting a heuristic approach. Results of computer simulations show that the proposed method is effective in the enhancement of RGB data. This paper is organized as follows. Section II describes the new three-output recursive enhancement system, Section III discusses the results of many computer simulations and, finally, Section IV reports conclusions.

II. RECURSIVE THREE-OUTPUT ENHANCEMENT SYSTEM

The proposed method deals with the 11-pixel neighborhood shown in Fig.1. The operation is composed of three processing steps dealing with the pixel subsets A (Fig.1a), B (Fig.1b) and C (Fig.1c), respectively. The first two steps perform detail-preserving filtering in the RGB color space. The third step operates in the $YCbCr$ [1] color coordinate system and applies the sharpening effect to the luminance channel only.

This work was supported by the University of Trieste, Trieste, Italy.
F. Russo is with the Department of Engineering and Architecture, University of Trieste, I-34127 Trieste, Italy (e-mail: rusfab@units.it).

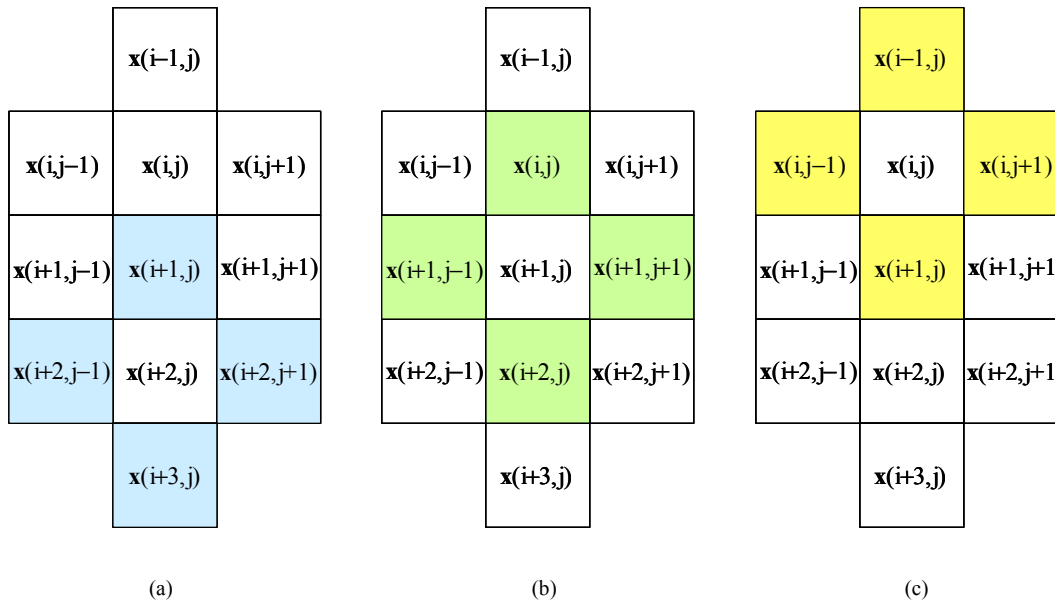


Fig.1 – Pixel subsets for multiple-output recursive processing: (a) pixel subset A, (b) pixel subset B, (c) pixel subset C.

A. Processing the pixel subset A

The first processing step performs detail-preserving smoothing of Gaussian noise. Let $\mathbf{x}(i+2,j)=[x_1(i+2,j), x_2(i+2,j), x_3(i+2,j)]^T$ be the vector (in the RGB space) representing the pixel at spatial position $(i+2,j)$ in the input noisy image ($i=1, \dots, N_1; j=1, \dots, N_2$), where x_1, x_2 and x_3 briefly denote the R, G and B components, respectively. Let each component be digitized by adopting Q different levels: $0 \leq x_k \leq Q-1$ ($Q=256$ for a 24-bit RGB color picture). Similarly, let $\mathbf{y}(i+2,j)=[y_1(i+2,j), y_2(i+2,j), y_3(i+2,j)]^T$ be the corresponding output of the processing, given by the following relationships:

$$y_k(i+2,j) = x_k(i+2,j) - g_k^{(A)}(i+2,j) \tag{1}$$

$$g_k^{(A)}(i+2,j) = \frac{1}{4} \sum_{\mathbf{x}(m,n) \in A} (x_k(i+2,j) - x_k(m,n)) \mu_{SI}(x_k(i+2,j), x_k(m,n), p_1, q_1) \tag{2}$$

where $g_k^{(A)}(i+2,j)$ is an estimate of the noise amplitude at location $(i+2,j)$ in the k -th channel and $\mu_{SI}(u,v,p,q)$ is the parameterized membership function that describes the fuzzy relation “ u is similar to v ”:

$$\mu_{SI}(u,v,p,q) = \begin{cases} 1 & |u-v| < p \\ \frac{pq - |u-v|}{(q-1)|u-v|} & p \leq |u-v| < pq \\ 0 & |u-v| \geq pq \end{cases} \tag{3}$$

where p and q are parameters ($0 < p < Q, q > 1$). An example of graphical representation of $\mu_{SI}(u,v,p,q)$ is depicted in Fig.2a. The processing defined by (1-3) is very simple. In order to reduce detail blur, the operation considers small pixel differences (possibly caused by Gaussian noise) and aims at excluding large differences that denote object borders. When all absolute differences between the central pixel and its neighbors are smaller than p , only noise is assumed to be present. Hence, the processing performs strong smoothing and the result is the arithmetic mean of the pixel values in the neighborhood. According to this model, differences larger than pq represent edges and then their contribution is zero. The shape of the membership function $\mu_{SI}(u,v,p,q)$ performs a gradual transition between these opposite effects. An appropriate choice of the parameter values p and q determines how much a pixel difference should be considered unwanted noise to be cancelled or useful information to be preserved. Typically, large noise variances require large values of the parameter p , at the price of a lower detail preservation. Conversely, the choice of the parameter q is much less critical and good results can be obtained in the range $3 \leq q < 8$. The processing is recursive, i.e., the new value $y(i+2,j)$ is immediately assigned to $x(i+2,j)$ and re-used for further processing.

B. Processing the pixel subset B

The second processing step deals with the pixel subset B centered on $\mathbf{x}(i+1,j)$ and reinforces the noise cancellation. It is worth pointing out that the pixel values in subset B are the results of previous processing. Indeed, the processing is recursive and the window scans the image from left to right and from top to bottom. The second operation performs

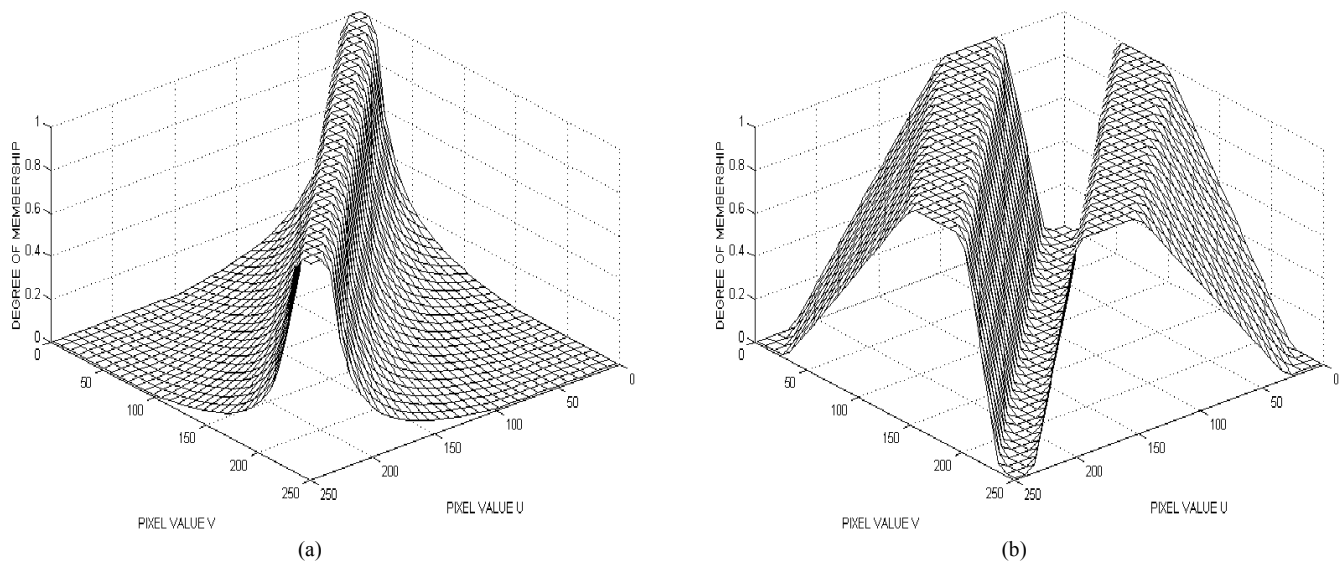


Fig.2 – Example of graphical representation of membership functions: (a) μ_{SI} ($p=15, q=10$), (b) μ_{DI} ($a=15, b=50, c=100, d=220$).

smoothing of prefiltered data and then the noise cancellation increases. Like the previous processing step, the output $y(i+1,j)=[y_1(i+1,j), y_2(i+1,j), y_3(i+1,j)]^T$ is defined by the following relationships:

$$y_k(i+1,j) = x_k(i+1,j) - g_k^{(B)}(i+1,j) \quad (4)$$

$$g_k^{(B)}(i+1,j) = \frac{1}{4} \sum_{x(m,n) \in B} (x_k(i+1,j) - x_k(m,n)) \mu_{SI}(x_k(i+1,j), x_k(m,n), p_2, q_2) \quad (5)$$

where $g_k^{(B)}(i+1,j)$ is an estimate of the noise amplitude at location $(i+1,j)$ in the k -th channel, The new value $y(i+1,j)$ is immediately assigned to $x(i+1,j)$ and re-used for further processing.

C. Processing the pixel subset C

The third processing step deals with the pixel subset C centered on $x(i,j)$ and performs detail sharpening. Let $x_L(i,j)$ be the luminance of the pixel at location (i,j) after conversion from the RGB to the $YCbCr$ color space. The output $y_L(i,j)$ is evaluated by means of the following relations:

$$y_L(i,j) = \text{MIN} \left\{ x_L(i,j) + \lambda f_L^{(C)}(i,j), Q-1 \right\} \quad (6)$$

where λ controls the amount of sharpening ($\lambda > 0$) and $f_L^{(C)}(i,j)$ is the output of the pseudo high-pass filter defined as follows:

$$f_L^{(C)}(i,j) = \frac{1}{4} \sum_{x_L(m,n) \in C} (x_L(i,j) - x_L(m,n)) \mu_{DI}(x_L(i,j), x_L(m,n), a, b, c, d) \quad (7)$$

where $\mu_{DI}(u,v,a,b,c,d)$ is defined by the following relationship:

$$\mu_{DI}(u,v,a,b,c,d) = \begin{cases} \frac{|u-v|-a}{b-a} & a \leq u-v < b \\ 1 & b \leq u-v < c \\ \frac{d-|u-v|}{d-c} & c \leq u-v < d \\ 0 & \text{otherwise} \end{cases} \quad (8)$$

and a, b, c, d are parameters: $a < b < c < d$.

The parameterized membership function $\mu_{DI}(u,v,a,b,c,d)$ describes the fuzzy relation “ u is different from v ”. We adopt this kind of fuzzy relation because sharpening aims at highlighting the differences among pixel values. An example of graphical representation of $\mu_{DI}(u,v,a,b,c,d)$ is reported in Fig.2b. It should be observed that the membership function shape is of paramount importance in providing the correct behavior of the sharpening effect. In particular, the sensitivity to noise depends upon the parameter a whereas the responses to small, medium and strong edges is controlled by the parameters b, c and d , respectively. The goal is to limit the noise increase, to strongly enhance small edges, to moderately enhance medium edges and not to enhance large edges in order to avoid annoying overshoots along the object borders. The parameter λ easily controls the overall amount of sharpening.

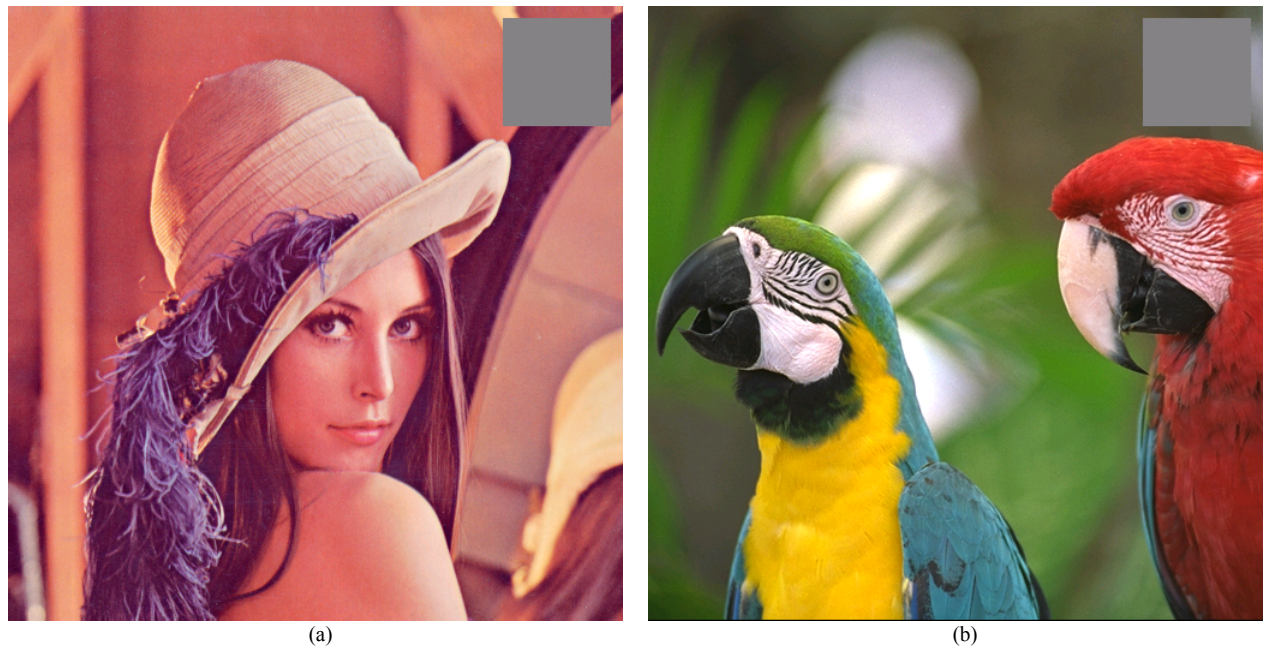


Fig.3 – Modified 24-bit RGB test pictures with superimposed uniform regions of interest (ROI) for noise measurements: (a) “Lena”, (b) “Parrots”.

III. COMPUTER SIMULATIONS

We performed many computer simulations in order to study how the behavior of the new enhancement system depends upon different parameter settings. In these experiments, we considered two 24-bit color images whose size is 512-by-512 pixels. We slightly modified the well-known test pictures “Lena” (Fig.3a) and “Parrots” (Fig.3b), superimposing a small uniform region ($R=G=B=128$) in the proximity of the upper right corner in order to ease the measurement of residual noise after sharpening.

We analyzed the effects of parameter settings on smoothing and sharpening.

A. Smoothing

In this first group of experiments we considered the effect of parameters p_1 , q_1 , p_2 and q_2 on noise cancellation. For the sake of simplicity, we considered $p_2=p_1$ and $q_1=q_2$. We set $\lambda=0$, in order to disable the sharpening and to focus on the smoothing only. A portion of the “Lena” image corrupted by Gaussian noise with variance $\sigma^2=100$ is depicted in Fig.4a. Examples of filtered data ($p_2=p_1$, $q_1=q_2=4$). are shown in Fig.4b ($p_1=5$), Fig.4c ($p_1=15$) and Fig.4d ($p_1=30$).

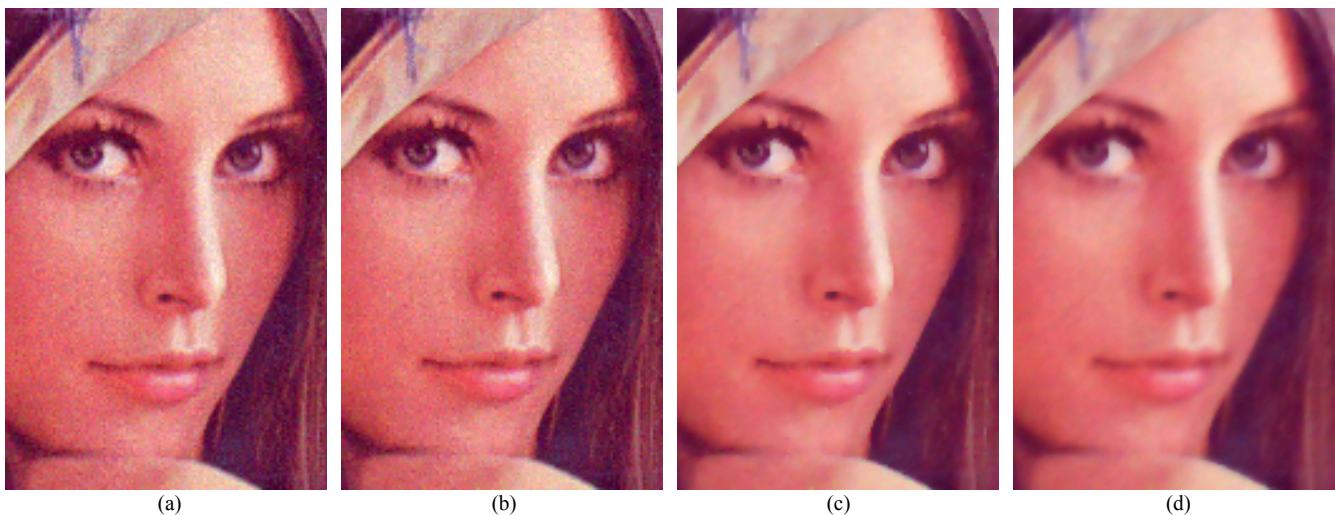


Fig.4 – (a) Portion of the “Lena” image corrupted by Gaussian noise with $\sigma^2=100$. Smoothing yielded by different choices of p_1 ($p_2=p_1$, $q_1=q_2=4$): (b) $p_1=5$ (CPSNR=29.15 dB, CPSBR=40.18), (c) $p_1=15$ (CPSNR=32.94 dB, CPSBR=35.30), (d) $p_1=30$ (CPSNR=31.19.15 dB, CPSBR=32.39).

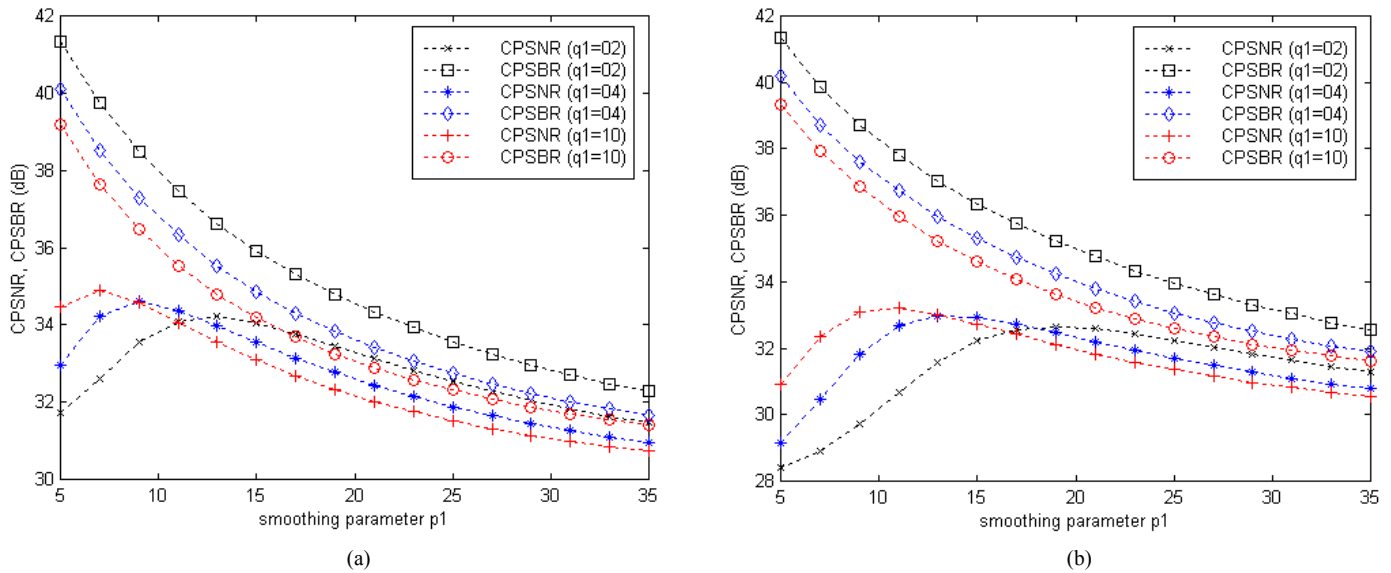


Fig.5 – CPSNR and CPSBR evaluations for different values of parameters p_1 and q_1 ($p_2=p_1$, $q_2=q_1$): (a) “Lena” image corrupted by Gaussian noise with $\sigma^2=50$, (b) “Lena” image corrupted by Gaussian noise with $\sigma^2=100$.

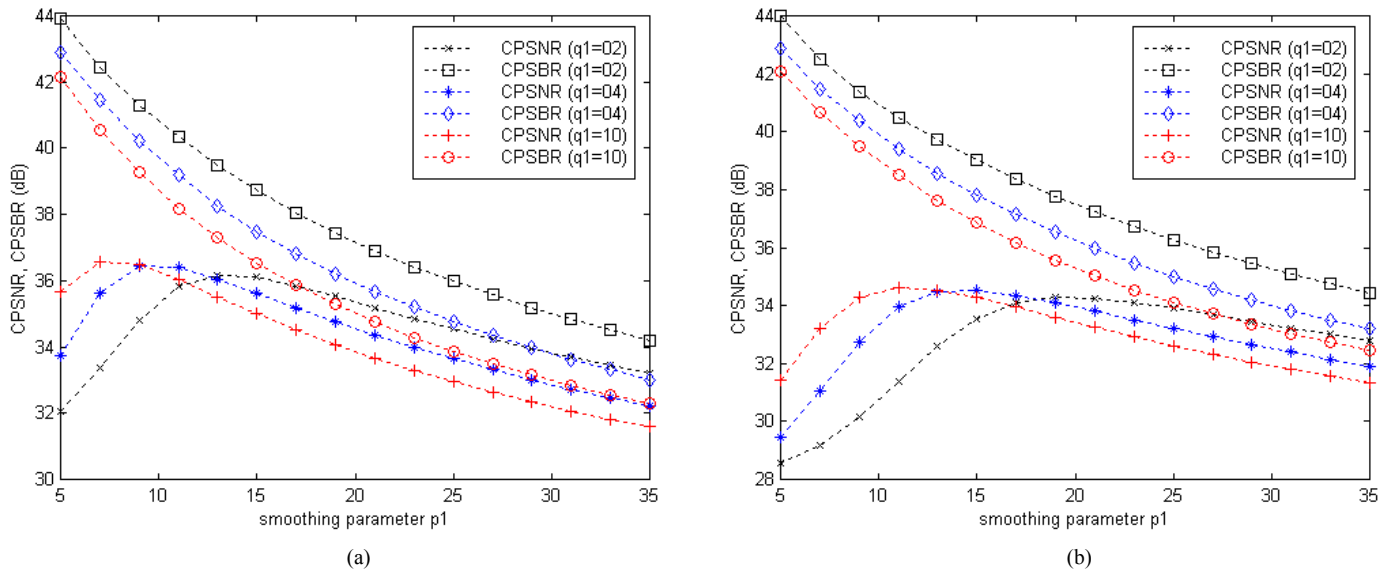


Fig.6 – CPSNR and CPSBR evaluations for different values of parameters p_1 and q_1 ($p_2=p_1$, $q_2=q_1$): (a) “Parrots” image corrupted by Gaussian noise with $\sigma^2=50$, (b) “Parrots” image corrupted by Gaussian noise with $\sigma^2=100$.

It can be seen that the removal of noise becomes more effective as the value of p_1 increases, at the price of some detail blur. In general, p_1 (and so p_2) strongly depend upon the noise variance σ^2 and a tradeoff between noise cancellation and detail preservation should be adopted. A quantitative evaluation of the filtering effects can be achieved by resorting to full-reference metrics such as the well-known *color peak signal-to-noise ratio* (CPSNR) and the recently introduced *color peak signal-to-blur ratio* (CPSBR) [28-29]. Since the CPSBR is the CPSNR

component that measures the color/detail preservation yielded by a color filter, it can be adopted in conjunction with the classical and widespread adopted CPSNR in order to fully characterize the behavior of a color denoising system. CPSNR and CPSBR evaluations for different choices of parameters p_1 and q_1 ($p_2=p_1$, $q_2=q_1$) are graphically depicted in Fig.5 (“Lena”) and Fig.6 (“Parrots”) for different values of noise variance. We can observe that larger values of q_1 typically yield lower values of CPSBR and so of detail preservation. On the other hand, too small

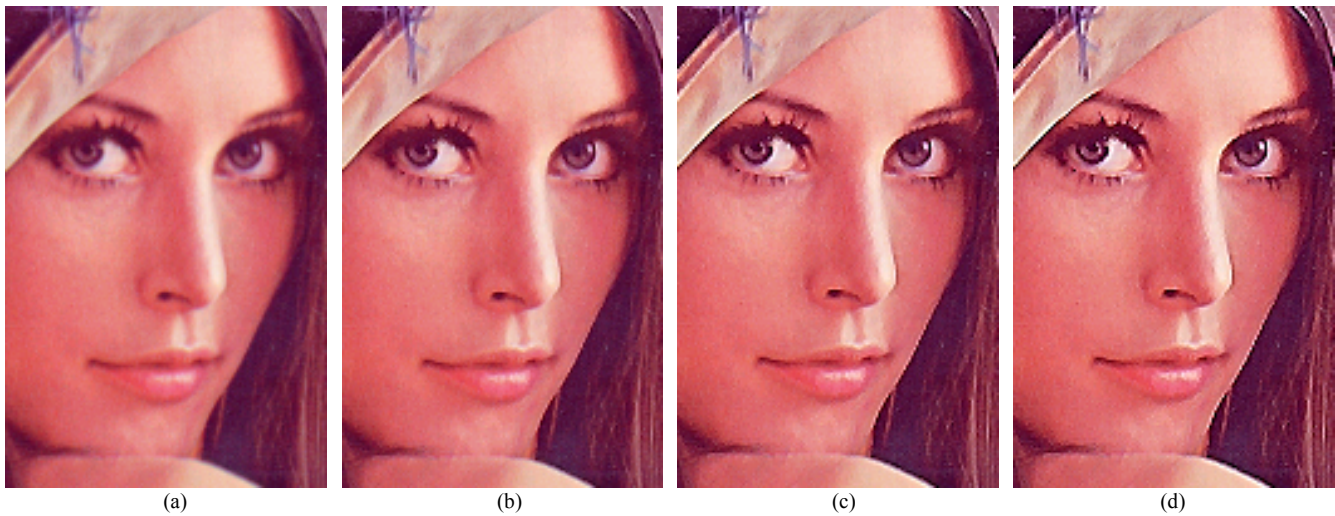


Fig.7 – Portion of the original noise-free “Lena” image (a), sharpening yielded by $\lambda=2$ (b), $\lambda=4$ (c), $\lambda=6$ (d).

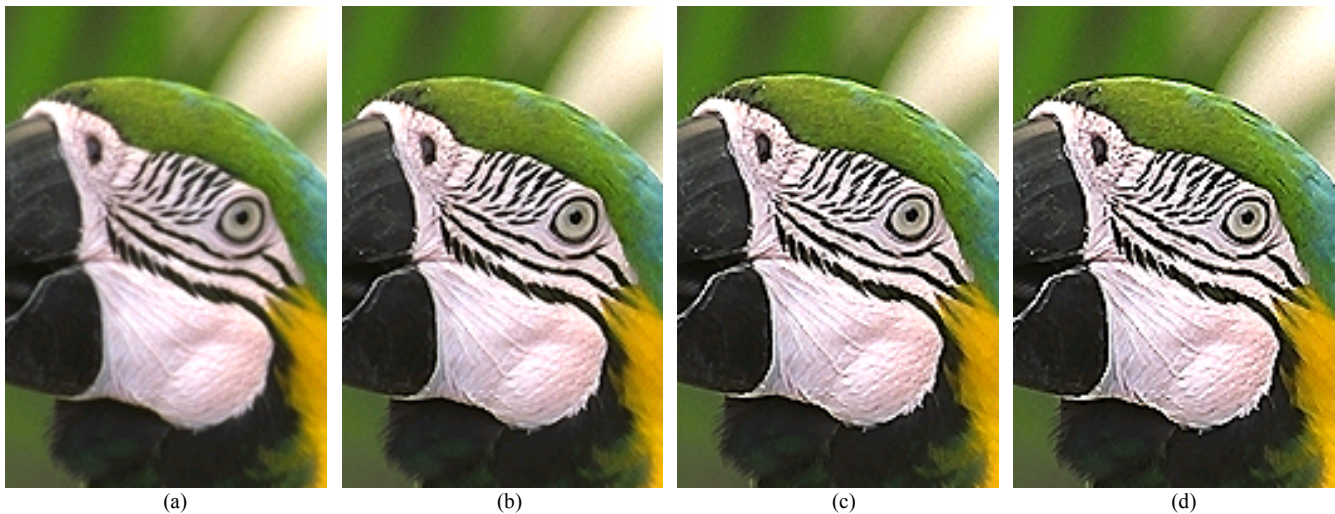


Fig.8 – Portion of the original noise-free “Parrots” image (a), sharpening yielded by $\lambda=2$ (b), $\lambda=4$ (c), $\lambda=6$ (d).

values of q_1 reduce the noise smoothing (the maximum CPSNR is lower). This effect should be carefully taken into account because the sharpening step might amplify the residual noise. For many applications, satisfactory choices can be found in the range $3 \leq q_1 < 8$ (for example, $q_1=4$).

B. Sharpening

According to (6-8), the behavior of the fuzzy sharpener is controlled by five parameters λ , a , b , c and d . We first considered the effect of the parameter λ on the sharpening effect. For this purpose, we chose noise-free input data and $p_1=p_2=0$ in order to focus on the sharpening only. For the sake of simplicity, we chose the following values for the remaining parameters: $a=0$, $b=50$, $c=100$, $d=150$. A portion of the original “Lena” image is depicted in Fig.7a. Examples of processed data are shown in Fig.7b ($\lambda=2$), Fig.7c ($\lambda=4$) and

Fig.7d ($\lambda=6$). Clearly, the detail sharpening becomes more effective as the value of λ increases. Too large values, however, typically generate excessive overshoot on object contours, although the proposed sharpening architecture is designed to limit this effect. Similar results are obtained using the “Parrots” picture (Fig.8). A portion of the original “Parrots” image is depicted in Fig.8a. Examples of processed data are shown in Fig.8b ($\lambda=2$), Fig.8c ($\lambda=4$) and Fig.8d ($\lambda=6$). The parameter a is very important because it controls the sensitivity to noise. Since small luminance differences are considered as noise, no sharpening ($\mu_{DI}=0$) is performed if $x_L(i,j)$ is not very different from $x_L(m,n)$, i.e., when $|x_L(i,j)-x_L(m,n)| < a$, according to (7-8). Large values of this parameter reduce noise amplification at the price of a (possibly) negligible enhancement of fine details. Conversely, too small values of the parameter a can significantly amplify

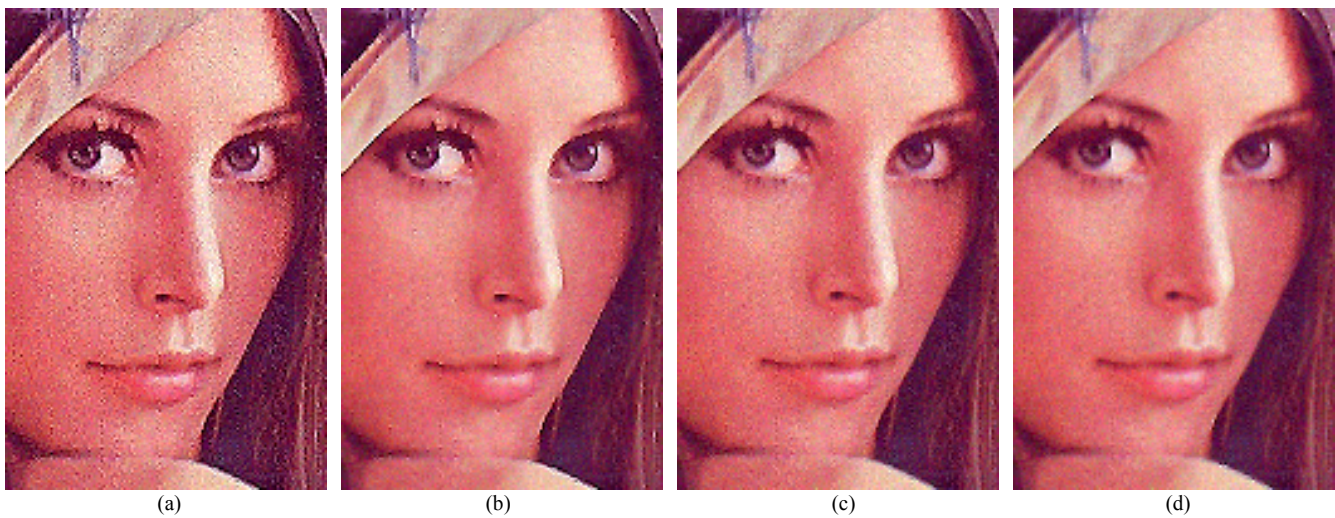


Fig.9 – Effects of sharpening parameters on a noisy input picture (“Lena” image corrupted by Gaussian noise with $\sigma^2=100$): (a) $a=0$, $b=50$, $c=100$, $d=150$, $\lambda=4$; (b) $a=30$, $b=50$, $c=100$, $d=150$, $\lambda=4$; (c) $a=60$, $b=80$, $c=100$, $d=150$, $\lambda=4$; (d) $a=0$, $b=200$, $c=225$, $d=250$, $\lambda=4$.

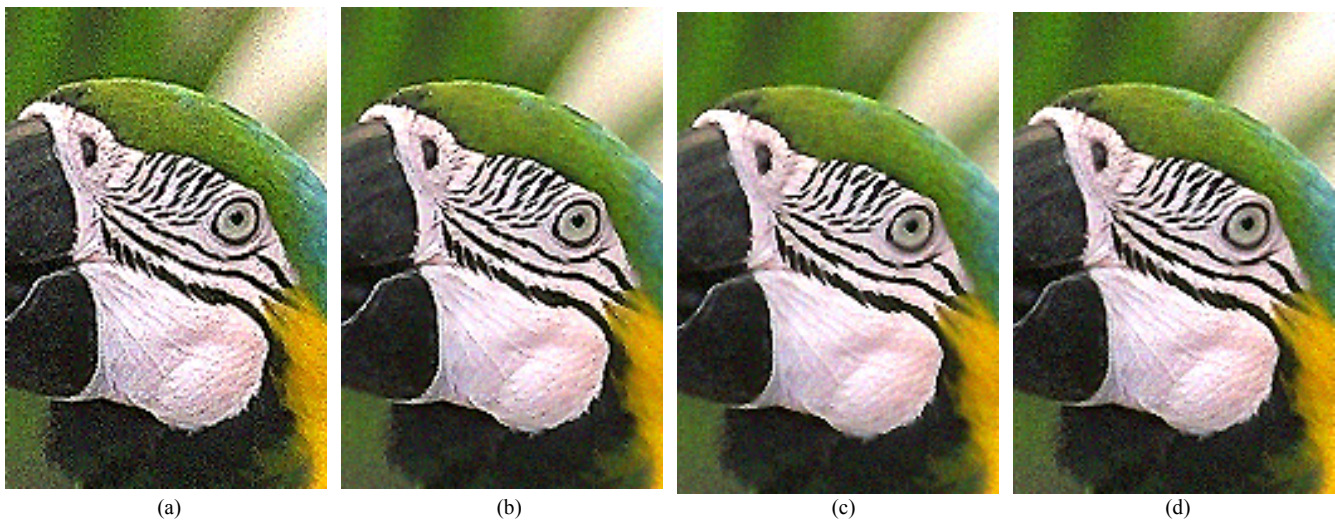


Fig.10 – Effects of sharpening parameters on a noisy input picture (“Parrots” image corrupted by Gaussian noise with $\sigma^2=100$): (a) $a=0$, $b=50$, $c=100$, $d=150$, $\lambda=4$; (b) $a=30$, $b=50$, $c=100$, $d=150$, $\lambda=4$; (c) $a=60$, $b=80$, $c=100$, $d=150$, $\lambda=4$; (d) $a=0$, $b=200$, $c=225$, $d=250$, $\lambda=4$.

the noise. A satisfactory choice can be easily achieved by aiming at a compromise between these opposite effects. As an example, let us consider again the “Lena” image corrupted by Gaussian noise with $\sigma^2=100$ (Fig.4a). Examples of correct and unsatisfactory parameter settings are depicted in Fig.9. (Notice that no noise attenuation can be obtained in any case). Focusing on the parameter a , we see that the choice $a=0$ (Fig.9a) is unsatisfactory for a noisy picture: the sharpening effect is activated ($\mu_{DI} \neq 0$) for any luminance difference, and the noise increase is apparent. Conversely, the choice $a=30$ (Fig.9b) can limit noise amplification and can sharpen many image details as well. A larger value of this parameter further decreases noise amplification. The price to be paid, however, is a strong limitation of detail enhancement (Fig.9c). The strength of the sharpening action actually depends on the slope of the membership function μ_{DI} , that is also determined by

parameters b , c and d . The parameter b (typically $b < 50$). controls the response to small-medium details that occur when $a < |x(i,j) - x(m,n)| \leq b$. A strong sharpening action is necessary in order to effectively highlight such details. Too large values of the parameter b should be avoided, because they could reduce the strength of the sharpening. An example is reported in Fig.9d ($a=0$, $b=200$), for visual inspection. We can see that the resulting contrast enhancement is more limited than for the data in Fig.9a ($a=0$, $b=50$). The choice of the remaining parameters c and d is not very critical too. They aim at avoiding an excess of overshoots along image edges, because this effect would be rather annoying. According to this idea, the sharpening is gradually disabled when the luminance differences become medium ($b < |x(i,j) - x(m,n)| \leq c$), large ($c < |x(i,j) - x(m,n)| \leq d$) and very large ($|x(i,j) - x(m,n)| > d$).

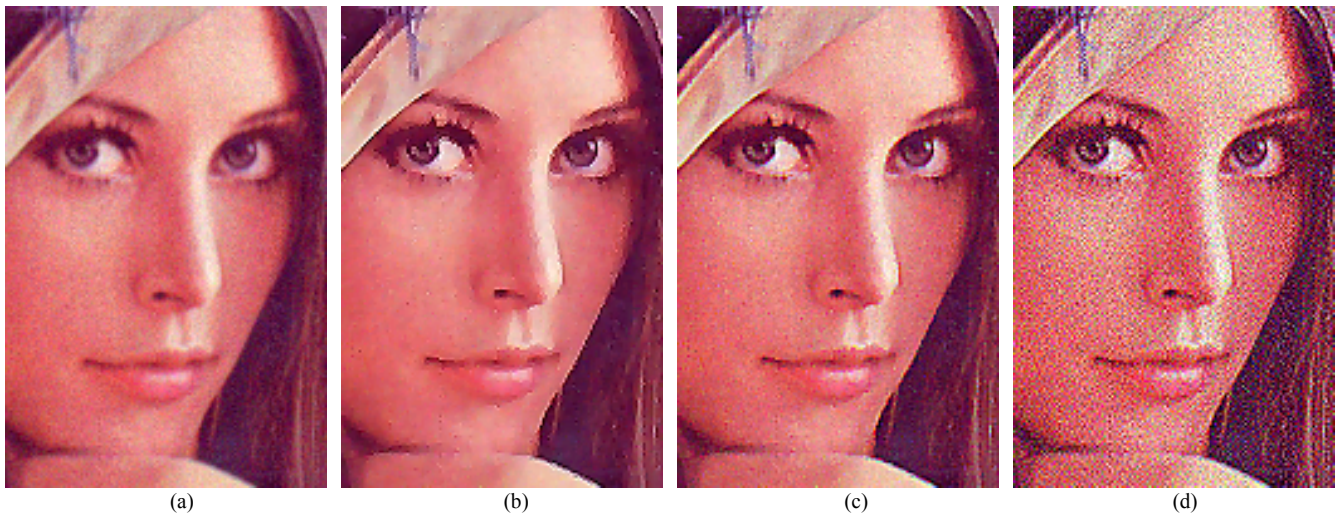


Fig.11 – Portion of the “Lena” image corrupted by Gaussian noise with variance $\sigma^2=80$ (a), results yielded by the proposed method (b), by our previous technique (c) and by the linear unsharp masking operator (d).

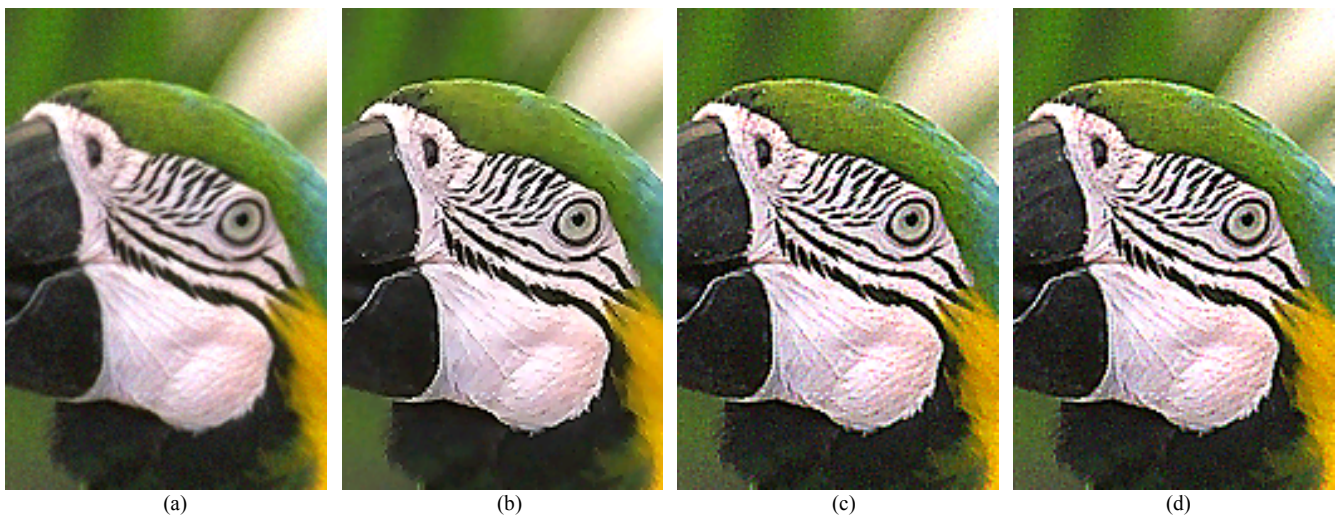


Fig.12 – Portion of the “Parrots” image corrupted by Gaussian noise with variance $\sigma^2=50$ (a), results yielded by the proposed method (b), by our previous technique (c) and by the linear unsharp masking operator (d).

C. Combining smoothing and sharpening

In this experiment we evaluated the performance of the complete operator in the presence of noisy image data. A portion of the (modified) “Lena” picture corrupted by Gaussian noise with variance $\sigma^2=80$ is depicted in Fig.11a. The result yielded by the novel enhancement system is shown in Fig.11b ($p_1=12, p_2=12, q_1=q_2=4, a=12, b=50, c=100, d=150, \lambda=3.5$). For a comparison, the results given by our previous fuzzy method [27] and by the classical linear unsharp masking technique are reported in Fig.11c and 11d, respectively. From visual inspection, we can see that the proposed method can perform edge enhancement and noise cancellation as well. On the contrary, some noise amplification affects the data processed by our previous technique. This effect becomes very annoying if we consider the result yielded

by the linear operator. A quantitative estimate of the resulting noise can be easily achieved by computing the CPSNR in the uniform region of interest (ROI) located at the upper-right corner of the modified test images. The CPSNR_{ROI} evaluations are: 39.51 dB (proposed method), 25.07 dB (previous technique [27]) and 15.35 dB (linear unsharp masking). Finally, we considered the (modified) “Parrots” picture corrupted by Gaussian noise with variance $\sigma^2=50$ (Fig.12a). The result given by the new enhancement system is shown in Fig.12b ($p_1=10, p_2=10, q_1=4, q_2=4, a=10, b=50, c=100, d=150, \lambda=3.5$). The results yielded by our previous fuzzy method [27] and by the classical linear unsharp masking technique are reported in Fig.12c and 12d, respectively. As in the previous experiment, we compute the CPSNR in the uniform ROI in order to obtain an estimate of the resulting

noise. The $CPSNR_{ROI}$ evaluations are 41.76 dB (proposed method), 24.53 dB (previous method) and 18.35 dB (linear unsharp masking technique).

IV. CONCLUSION

A new operator for contrast enhancement of color images has been presented. The proposed approach adopts recursive processing based on fuzzy models in order to combine edge sharpening and noise reduction. Edge-preserving noise smoothing is directly performed on RGB data, whereas detail sharpening operates on the luminance channel of the image in order to avoid chroma distortion. Unlike other methods, the processing can be finely adjusted by acting on many parameters. The parameter tuning, however, is not a critical process: indeed satisfactory results can be easily achieved focusing on few parameter settings. Computer simulations dealing with 24-bit RGB pictures have shown that the novel fuzzy operator can effectively sharpen image details and reduce noise, yielding better results than other methods in the literature.

REFERENCES

- [1] R.C. Gonzalez, R.E. Woods, *Digital Image Processing*, Pearson International, London, 2008.
- [2] A. K. Jain, *Fundamentals of Digital Image Processing*, Prentice-Hall, Englewood Cliffs, 1989.
- [3] G. Ramponi, "Polynomial and rational operators for image processing and analysis", in S.K Mitra and G. Sicuranza (eds.) *Nonlinear Image Processing*, Academic, London, 2000, pp.203–223.
- [4] G.R. Arce, J.L. Paredes, "Image enhancement and analysis with weighted medians", in S.K Mitra and G. Sicuranza (eds.) *Nonlinear Image Processing*, Academic, London, 2000, pp. 27–67.
- [5] S.C. Matz, R.J.P. de Figueiredo, "A nonlinear technique for image contrast enhancement and sharpening". *Proc. IEEE ISCAS*, 1999, pp. 175–178.
- [6] S.C. Matz, R.J.P. de Figueiredo, "Exponential nonlinear Volterra filters for contrast sharpening in noisy images", *Proc. IEEE ICASSP*, 1996, pp. 2263–2266.
- [7] A. Polesel, G. Ramponi, V.J. Mathews, "Image enhancement via adaptive unsharp masking". *IEEE Trans. Image Process.* vol.9, n.3, 2000, pp.505–510.
- [8] R.C. Hardie, K.E. Barner, "Extended permutation filters and their application to edge enhancement", *IEEE Trans. Image Process.* vol.5, n.6, 1996, pp.855–867.
- [9] M. Fischer, J.L. Paredes, G.R. Arce, "Image sharpening using permutation weighted medians", *Proc. X EUSIPCO*, Tampere, Finland, 2000, pp. 299–302.
- [10] M. Fischer, J.L. Paredes, G.R. Arce, "Weighted median image sharpeners for the World Wide Web". *IEEE Trans. Image Process.* vol.11, n.7, 2002, pp.717–727.
- [11] S.K. Mitra, H.Li, I.-S. Lin, T.-H. Yu, "A new class of nonlinear filters for image enhancement", *Proc. Int. Conf. Acoust., Speech Signal Process*, Toronto, ON, Canada, 1991, pp. 2525–2528.
- [12] S. Thurnhofer, "Two-dimensional teager filters", in S.K Mitra and G. Sicuranza (eds.) *Nonlinear Image Processing*, Academic, London, 2000, pp.167–202.
- [13] G. Ramponi, N. Strobel, S.K. Mitra, T.-H. Yu, "Nonlinear unsharp masking methods for image contrast enhancement", *J. Electron. Imaging* vol.5, n.3, 1996, pp.353–366.
- [14] M. Nakashizuka and I. Aokii, "A cascade configuration of the cubic unsharp masking for noisy image enhancement", in *Proc. Int. Symp. Intell. Signal Process. Commun. Syst.*, Hong Kong, 2005, pp.161–164.
- [15] G. Ramponi, A. Polesel, "A rational unsharp masking technique", *J. Electron. Imaging* vol.7, n.2, 1998, pp.333–338.
- [16] F. Russo, "Automatic Enhancement of Noisy Images Using Objective Evaluation of Image Quality", *IEEE Trans. on Instrumentation and Measurement*, vol. 54, n.4, 2005, pp.1600–1606.
- [17] F. Russo, "An Image Enhancement System Based on Noise Estimation", *IEEE Trans. Instrum. Meas.* vol.56, n.4, 2007, pp.1435–1442.
- [18] C. Gatta, P. Radeva, "Bilateral enhancers", *Proc. 2009 IEEE International Conference on Image Processing, ICIP 2009*, pp.3161–3164.
- [19] A. Choudhury and G. Medioni, "Perceptually Motivated Automatic Sharpness Enhancement Using Hierarchy of Non-Local Means", *Proc. 2011 IEEE International Conference on Computer Vision*, pp.730–737.
- [20] G. Gilboa, N. Sochen, and Y. Y. Zeevi, "Forward-and-Backward Diffusion Processes for Adaptive Image Enhancement and Denoising", *IEEE Trans. on Image Proc.* Vol.11, n. 7, 2002, pp.689–703.
- [21] S. Bettahar, A. B. Stambouli, P. Lambert and A. Benoit, "PDE-Based Enhancement of Color Images in RGB Space", *IEEE Trans. on Image Proc.*, vol. 21, n.5, 2012, pp.2500–2512.
- [22] S. Bettahar, P. Lambert, A. B. Stambouli, "Anisotropic Color Image Denoising and Sharpening", *IEEE ICIP 2014*, pp.2669–2673.
- [23] K.-W. Lee et al. , "Effective Color Distortion and Noise Reduction for Unsharp Masking in LCD", *IEEE Trans. on Consumer Electronics*, vol. 54, n.3, 2008, pp.1473–1477.
- [24] M. Wirth and D. Nikitenk, "The effect of colour space on image sharpening algorithms", *2010 Canadian Conference on Computer and Robot Vision*, pp.79–85.
- [25] A. Alsam, "Colour Constant Image Sharpening", *Proc. 2010 IEEE International Conference on Pattern Recognition*, pp.4524–4568.
- [26] F. Russo, "An image enhancement technique combining sharpening and noise reduction", *IEEE Trans. Instrum. Meas.*, vol.51, n.4, 2002, pp.824–828.
- [27] F. Russo, "Design of Fuzzy Relation-Based Image Sharpeners", in A. Ruano and A. Varkonyi-Koczy (Eds.): *New Advances in Intelligent Signal Processing, SCI 372*, Springer-Verlag Berlin Heidelberg, 2011, pp. 115–131.
- [28] F. Russo, "New Tools for Classification and Evaluation of Filtering Errors in Color Image Denoising", *International Journal of Circuits, Systems and Signal Processing*, Vol.10, 2016, pp.178–189, ISSN 1998-4464.
- [29] F. Russo, "Study of the Accuracy of the Color Peak Signal-to-Blur Ratio (CPSBR)", *International Journal of Circuits, Systems and Signal Processing*, Vol.10, 2016, pp. 242–253, ISSN 1998-4464.

F. Russo is currently Associate Professor of electrical and electronic measurements in the Department of Engineering and Architecture of the University of Trieste, Italy. He is author/coauthor of more than 100 papers in international journals, textbooks, and conference proceedings including the Wiley Encyclopedia of Electrical and Electronics Engineering. (J. G. Webster ed.). His research interests presently include nonlinear and fuzzy techniques for image denoising, image enhancement and image quality measurement. He was one of the organizers of the 2004 and 2005 IEEE International Workshops on Imaging Systems and Techniques. He served as Technical Program Co-Chairman of the 2006 IEEE Instrumentation and Measurement Technology Conference and as Co-Guest Editor for the Special Issue of the IEEE Transactions on instrumentation published in August 2007. He was invited speaker of the plenary session "Fuzzy Models for Low-level Computer Vision: a Comprehensive Approach" at the IEEE Symposium on Intelligent Signal Processing (WISP 2007). He has served as session chairman/co-chairman in many conferences organized by IEEE, IMEKO, WSEAS and NAUN.